



## Impaired adhesion of neutrophils expressing Slc44a2/HNA-3b to VWF protects against NETosis under venous shear rates

Gaïa Zirka, Philippe Robert, Julia Tilburg, Victoria Tishkova, Chrissta Maracle, Paulette Legendre, Bart van Vlijmen, Marie-Christine Alessi, Peter Lenting, Pierre-Emmanuel Morange, et al.

### ► To cite this version:

Gaïa Zirka, Philippe Robert, Julia Tilburg, Victoria Tishkova, Chrissta Maracle, et al.. Impaired adhesion of neutrophils expressing Slc44a2/HNA-3b to VWF protects against NETosis under venous shear rates. *Blood*, 2021, 137 (16), pp.2256-2266. 10.1182/blood.2020008345 . hal-03295352

**HAL Id: hal-03295352**

**<https://amu.hal.science/hal-03295352>**

Submitted on 9 May 2023

**HAL** is a multi-disciplinary open access archive for the deposit and dissemination of scientific research documents, whether they are published or not. The documents may come from teaching and research institutions in France or abroad, or from public or private research centers.

L'archive ouverte pluridisciplinaire **HAL**, est destinée au dépôt et à la diffusion de documents scientifiques de niveau recherche, publiés ou non, émanant des établissements d'enseignement et de recherche français ou étrangers, des laboratoires publics ou privés.



Distributed under a Creative Commons Attribution - NonCommercial 4.0 International License

## **Impaired adhesion of neutrophils expressing Slc44a2/HNA-3b to VWF protects against NETosis under venous shear rate**

Gaïa Zirka,<sup>1</sup> Philippe Robert,<sup>2,3</sup> Julia Tilburg,<sup>4</sup> Victoria Tishkova,<sup>5</sup> Chrissta X. Maracle,<sup>4</sup> Paulette Legendre,<sup>6</sup> Bart J.M. van Vlijmen,<sup>4</sup> Marie-Christine Alessi,<sup>1,7</sup> Peter J. Lenting,<sup>6</sup> Pierre-Emmanuel Morange<sup>1,7</sup> and Grace M. Thomas<sup>1</sup>

<sup>1</sup>Aix-Marseille Univ, INSERM, INRAE, C2VN, Marseille, France,

<sup>2</sup>Aix Marseille Univ, CNRS, INSERM, LAI, Marseille, France,

<sup>3</sup>APHM, CHU de la Conception, Laboratoire d'immunologie, Marseille, France,

<sup>4</sup>Eindhoven Laboratory for Experimental Vascular Medicine, Division of Thrombosis and Hemostasis, Department of Internal Medicine, Leiden University Medical Center, Leiden, the Netherlands,

<sup>5</sup>Aix Marseille Univ, CNRS, CInaM, Marseille, France,

<sup>6</sup>Inserm, UMR-S 1176, Université Paris-Sud, Université Paris-Saclay, Le Kremlin- Bicêtre, France,

<sup>7</sup>APHM, CHU de la Timone, Laboratoire d'hématologie, Marseille, France

### **Corresponding author:**

Grace M THOMAS

Inserm UMR\_S1263 Center for CardioVascular and Nutrition Research - C2VN

Faculté de médecine Timone, 3eme étage aile bleue

27 Bd Jean Moulin

13385 Marseille CEDEX 05 France

Email: [grace.thomas@univ-amu.fr](mailto:grace.thomas@univ-amu.fr)

Phone: +33 (0)491324674

Fax: +33 (0)491254336

**Scientific category:** Vascular biology

**Keywords:** Slc44a2, CTL-2, Venous thrombosis, adhesion, cell activation, neutrophils, VWF, NETs

### **Key points**

- Slc44a2 expressed by neutrophils is important for their adhesion to VWF-A1 domain and can mediate NETosis on VWF at venous shear.
- Slc44a2 importance in neutrophil recruitment on VWF is exacerbated during inflammation both *in vitro* and *in vivo*

## Abstract

Genome wide association studies linked expression of the human neutrophil antigen 3b (HNA-3b) epitope on the Slc44a2 protein with a 30% decreased risk of venous thrombosis (VT) in humans. Slc44a2 is a ubiquitous transmembrane protein identified as a receptor for Von Willebrand factor (VWF). To explain the link between Slc44a2 and VT we wanted to determine how Slc44a2 expressing either HNA-3a or HNA-3b on neutrophils could modulate their adhesion and activation on VWF under flow.

Transfected HEK293T cells or neutrophils homozygous for the HNA-3a- or the HNA-3b-coding allele were purified from healthy donors and perfused in flow chambers coated with VWF at venous shear rates ( $100\text{s}^{-1}$ ). HNA-3a expression was required for Slc44a2-mediated neutrophil adhesion to VWF at  $100\text{s}^{-1}$ . This adhesion could occur independently of  $\beta_2$  integrin and was enhanced when neutrophils are preactivated with lipopolysaccharide (LPS). Moreover, specific shear conditions with high neutrophil concentration could act as a “second hit”, inducing the formation of neutrophil extracellular traps. Neutrophil mobilization was also measured by intravital microscopy in venules from *SLC44A2*-knockout and wild-type mice after histamine-induced endothelial degranulation. Mice lacking Slc44a2 showed a massive reduction in neutrophil recruitment in inflamed mesenteric venules.

Our results show that Slc44a2/HNA-3a is important for the adhesion and activation of neutrophils in veins under inflammation and when submitted to specific shears. Neutrophils expressing Slc44a2/HNA-3b not being associated with these observations, these results could thus explain the association between HNA-3b and a reduced risk for VT in humans.

## Introduction

Venous thromboembolic (VT) disease is the third cause of cardiovascular death after myocardial infarction and stroke in industrialized countries. VT is a multifactorial disease which mechanisms still remained to be fully uncovered. Until recently, pathophysiology of VT was only based on the original cascade model of coagulation. Accumulating data have highlighted mechanisms independent of coagulation cascade on clot formation.

Using genome wide association study (GWAS) approaches and transgenic mice our team and others have contributed to the identification of *SLC44A2* as a new gene involved with VT both in humans<sup>1,2</sup> and in mice.<sup>3-5</sup> In-depth analysis of the *SLC44A2* locus identified rs2288904 (461G>A; Arg154Gln) as the functional variant responsible for the association with VT. This polymorphism defines the expression of the human neutrophil antigen-3a (HNA-3a; 461G; Arg154) or HNA-3b antigen (461A; Gln154) by the choline transporter-like protein 2 (CTL-2, also called Slc44a2 protein) encoded by the *SLC44A2* gene.<sup>6-8</sup> Homozygosity for the HNA-3b-coding allele is associated with a decreased risk of VT of ~30%.<sup>1</sup>

Slc44a2 is an ubiquitous transmembrane protein of 70-95kDa<sup>9</sup> that has been identified in 2015 as a new receptor for Von Willebrand factor (VWF).<sup>10</sup> and in 2020 as a receptor for VWF-primed platelets through  $\alpha_{IIb}\beta_3$  interaction.<sup>11</sup> Slc44a2 has been associated with transfusion acute-lung injury (TRALI) which is one of the leading cause of transfusion-associated mortality in developed countries.<sup>12</sup> Severe cases have been associated with alloantibodies reacting against the Slc44a2/HNA-3a epitope, the same antigen associated to VT. We and others have shown that alloantibodies targeting Slc44a2 can lead to neutrophil activation and formation of neutrophil extracellular traps (NETs) by primed HNA-3a<sup>+</sup> neutrophils.<sup>13,14</sup> Platelet and neutrophil recruitment to the endothelium and neutrophil cell activation/NETosis are key steps in TRALI<sup>14,15</sup> but also in arterial thrombosis<sup>16</sup> and VT.<sup>17-19</sup> After adhesion to the activated endothelium, neutrophils initiate and propagate VT by interacting with platelets and by exposure of tissue factor and active FXII.<sup>18</sup> Importantly, mice with impaired NETosis have a decreased incidence of thrombosis in a model of VT,<sup>20</sup> and mice treated with DNase-1 (which degrades DNA and NETs) are protected in this model.<sup>17</sup> As for thrombosis, outcome of mice with TRALI could be improved by DNase-1 inhalation<sup>14</sup> The TRALI model, may pave the way to understand why Slc44a2 plays a role in VT and why the HNA-3b isoform carrier have a decreased risk of VT. We investigated in this study whether Slc44a2 could act as an adhesion protein allowing neutrophil adhesion to VWF under

flow, and whether Slc44a2 could act as a receptor able to activate neutrophils and stimulate NETosis.

We demonstrated that Slc44a2 is important in the adhesion and activation process of neutrophils under flow when submitted to inflammation and specific shear conditions. The fact that neutrophils expressing Slc44a2/HNA-3b show reduced rolling and activation on VWF, could thus explain the association between the HNA-3b epitope and the reduced risk for VT in humans.

## Methods

### Cell lines and culture

HEK293T cells stably transfected to express Slc44a2/HNA-3a (R154) or Slc44a2/HNA-3b (Q154) fused with a GFP tag were generous gifts from Prs. Daniel Bougie and Brian Curtis from the Bloodcenter of Wisconsin. Cells were cultured as previously described.<sup>8,21</sup> PBS and Versene (0.48 mM, Gibco) were used for cell dissociation.

### Human neutrophil isolation

After all participants gave written informed consent, neutrophils were isolated from healthy volunteers' blood at the Timone University Hospital (Marseille, France) who declared that they had not received any medication for at least 2 weeks. Sodium citrate was used as anticoagulant for blood puncture except if otherwise specified. Neutrophils were prepared as previously described.<sup>14</sup> The research was approved by the relevant institutional review boards and ethic committees. The investigation conforms to the principles outlined in the Declaration of Helsinki. After isolation, neutrophils were eventually labeled with the fluorescent dye of use. When specified, 1mM CaCl<sub>2</sub> and/or blocking antibodies were added to neutrophils before utilization. Concentration was adjusted and only cells at acceptable viability (>75%) were used.

### SLC44A2 genotyping

Donors homozygous for the HNA-3a- or HNA-3b-coding allele were identified by SNP genotyping using a taqman 5' exonuclease PCR technology as previously described.<sup>22</sup>

### Flow chamber assays

Flow chambers  $\mu$ -slide VI 0.1 ibitreat (Ibidi®) were used for cell velocity analysis and NETosis experiments. Vena8 fluoro + microfluidic biochip (Cellix®) were used for NETosis experiments. Chambers were coated overnight at 4°C with either 70  $\mu$ g/ml VWF (Wilfactin, LFB), VWF recombinant A1-Fc domain (10  $\mu$ g/ml), fibrinogen (10 $\mu$ g/ml), or BSA (10 $\mu$ g/ml, Sigma). Saturation was done with PBS/BSA 0.1% 1 hour prior to the assay. If applicable, blocking antibodies (10  $\mu$ g/ml; VWF-A1 blocking Ab 318 clone, anti-CD18 TS1/18 clone, irrelevant IgG1 or IgG2) were incubated in the channels and with neutrophils 30 minutes before cell perfusion and perfused concomitantly at 25 $\mu$ g/ml for VWF blockade experiments. Continuous flow rate was applied forward using an electrical syringe pump (bioblock

scientific), a Terumo syringe and silicon tubing. One channel was used per condition and the chambers were discarded after each experiment.

HEK293T cells or purified neutrophils were labeled 20 minutes under gentle agitation with either Calcein AM (4 $\mu$ M, Invitrogen), Cell trace red orange (4 $\mu$ M, Invitrogen) or DiD dye (2 $\mu$ g/ml) for experiments including cell activation. Cells were washed from the dye excess after staining. When indicated, neutrophils were incubated with lipopolysaccharide (LPS 5 or 25 $\mu$ g/ml) or MnCl<sub>2</sub> (1mM) for 1 hour prior to cell perfusion and eventually incubated 5 min before the experiment with calcium (1mM). Extracellular DNA was labeled by addition of Sytox green or Sytox red (1 $\mu$ M, Invitrogen) to the neutrophils immediately before perfusion. 1.5.10<sup>6</sup> cells/ml (or other if specified) were infused in flow chamber at a wall shear rate of 100s<sup>-1</sup> (or other if specified) at a controlled temperature of 37°C using a thermoregulated thermostatic chamber (Olympus). Cells were allowed to pass through the channel for 5 minutes before acquisition. For immunostaining experiments, neutrophils accumulated at the entrance of the chamber after perfusion at 100s<sup>-1</sup> were fixed using zinc fixative. Non-specific binding sites were blocked with Tween/BSA and cells were stained overnight at 4° for myeloperoxidase (mouse monoclonal IgG anti-human MPO, Abcam, 2 $\mu$ g/ml) and citrullinated histone H3 (rabbit polyclonal anti-human H3cit, Abcam, 2 $\mu$ g/ml). Goat anti-rabbit IgG-Alexa Fluor® 488 and goat-anti-mouse IgG-Alexa Fluor® 647 (Invitrogen, 4 $\mu$ g/ml) were used as secondary antibodies. Irrelevant antibodies were used for negative control (Mouse IgG from Biolegend and rabbit IgG from Abcam, 2 $\mu$ g/ml). Hoechst 33342 (1 $\mu$ g/ml) was used for DNA staining. Acquisition was done with an inverted microscope (IX71, Olympus) and a LED fluorescence lamp for sample excitation (SPECTRA X light engine, Lumencor) in 3 different fields (1329.4 $\mu$ m wide) during 1 minute at a rate of 50 images/sec. Real-time imaging was performed using a CMOS digital camera (Orca-Flash 4.0 V2 CCD C11440, Hamamatsu).

#### Flow chamber cell motion analysis

A dedicated program was written in Java (Oracle, USA) as a plug-in for ImageJ (NIH, USA). More details are given in supplementary material.

#### NET generation *in vitro*

NET generation was done and quantified as previously described.<sup>14</sup> Tumor necrosis factor- $\alpha$  (TNF $\alpha$ ) was used for cell priming because TNF- $\alpha$  is produced by human neutrophils stimulated by LPS<sup>23</sup> and also because it has been commonly used for this assay in other studies.

### Model of endothelial degranulation on mouse mesenteric venules

12-week-old *SLC44A2* knockout (KO) male mice (C57BL/6J background) and wild type littermate controls were used to investigate neutrophil recruitment upon endothelial degranulation as previously done.<sup>20</sup> Experimental animal procedures were approved by local welfare committees in Aix-Marseille University. Experiments were performed blinded for genotype. More details are given in supplementary material.

### Numerical simulations:

Numerical simulations were realized in finite elements (Comsol Multiphysics) in two steps. First, a stationary study of the fluid flow is performed in order to solve Navier-Stokes equation. The following parameters were used: fluid was considered as water, with water density and viscosity at 37°C, as protein and ion-induced changes are non-significant at physiological concentrations. Fluid velocity at wall contact was zero. Flow was identical at what was experimentally set for cell experiments (4µl/min for Cellix® chambers, 10µl/min for Ibidi® chambers). Dimensions of the chambers were given by respective manufacturers. Second, trajectories for each cell in the fluid were calculated and gravity was taken into account. A time-dependent study was performed for 60 sec. Cells were represented by spheres of radius 10µm and density 1.08, corresponding to the average human polymorphonuclear size and density. Each contact of a cell with the considered wall was counted as 1.

### Statistical analysis

Shapiro-Wilk test was used to check normality. Immunofluorescence data were analyzed with one-way ANOVA test, rolling data with nested t-test, NETosis quantification and *in vivo* data were analyzed with unpaired t test. Results were considered significant if  $p < 0.05$ .

## Results

### The Slc44a2/HNA-3a epitope is necessary for cell adhesion to VWF under flow

We used HEK293T cells expressing either Slc44a2/HNA-3a (Arg154) or Slc44a2/HNA-3b (Gln154). These cells have been already characterized and have been shown to express similar levels of Slc44a2<sup>8</sup> (verified by western-blot by detecting Slc44a2-co-expressed GFP, **Suppl. figure 1**). After co-incubation of cells with purified VWF, we observed patches positive for VWF staining 2.6-fold more intense on HEK293T/HNA-3a<sup>+</sup> than on HEK293T/HNA-3b<sup>+</sup> cells (**Figure 1**). We then perfused fluorescent transfected HEK293T cells in flow chambers pre-coated with VWF and submitted to a “postcapillary venule” shear rate of 100s<sup>-1</sup>. Digital real time imaging of the flowing cells allowed digital analysis of the velocity data. We plotted the frequency distribution of cell velocities from each of the 3 different fields analyzed. We observed a maximum of cells around 1400-1600μm/s (**Figure 2A**) corresponding to the non-sedimented population for both groups. We also detected some cells interacting strongly with the matrix (speed <10μm/s) in the HNA-3a<sup>+</sup> group. We compiled the cell velocities in 2 different populations: “Slow rolling” (<10μm/s) and “Rolling” (200-500μm/s). Exposure of HNA-3a by HEK293T cells allowed cell adhesion/slow rolling to the VWF matrix under flow, whereas HEK293T/HNA-3b<sup>+</sup> cells lost this ability (1.32 ± 0.60% against 0% of total tracked cells adhering to the matrix respectively, **Figure 2B**).

We wondered if Slc44a2 could also modulate neutrophil recruitment to VWF, which is crucial in VT. We repeated the previous experiment by replacing HEK293T cells with purified blood neutrophils from donors homozygous for either the HNA-3a- or the HNA-3b coding allele. As expected, we found the majority of the neutrophils as non-sedimented with an approximative speed of 1500-1600 μm/s. We also observed cells rolling at a speed around 300μm/s (**Figure 2C**). Here again, the HNA-3a/3b epitope did not influence the “Rolling” population on VWF, whereas HNA-3b<sup>+</sup> neutrophils showed a significant reduction in the “Slow rolling” population on this matrix (**Figure 2D, Suppl. Videos 1 and 2**). This was not observed in presence of higher shear rates (1000s<sup>-1</sup>, data not shown). We could inhibit HNA-3a-dependent adhesion with a specific VWF-A1 domain blocking antibody (**figure 2E**). These data suggest that the HNA-3b epitope expressed by Slc44a2 may reduce cell adhesion to VWF under venous shear rates.

### Neutrophil adhesion on VWF under flow is amplified after an inflammatory first “hit”

Inflammatory-related disorders often follow the two/multiple-hit hypothesis. HNA-3a-associated VT probably follows this pattern, and this may explain why not all the HNA-3a<sup>+</sup> population will suffer from VT. The difference between the HNA-3a<sup>+</sup> and HNA-3b<sup>+</sup> groups was also present when lower shear rates were applied (50 and 10s<sup>-1</sup>, **Figure 3A**) with a significant increase in the “slow rolling” population for HNA-3a<sup>+</sup> cells alone. We also tested an inflammatory hit mimicking an infection. We pre-activated neutrophils with LPS (5 or 25μg/ml) for 1 hour before perfusion. Since neutrophils lose their capacity to retain Calcein dyes during activation,<sup>24</sup> we stained the cells with a lipophilic membrane dye to permit cell tracking after LPS challenge. Our data show that LPS increases slow rolling of HNA-3a<sup>+</sup> neutrophil on VWF at 100s<sup>-1</sup> whereas HNA-3b<sup>+</sup> neutrophils seem to not be affected by LPS challenge (**Figure 3B**). LPS did not affect rolling for the 200-500μm/s velocity range (**Figure 3C**). This increase in cell adhesion suggested an integrin-dependent process. Because β<sub>2</sub> integrins can bind VWF, we assessed their contribution in our model without inflammatory stimulation. We treated HNA-3a/HNA-3b<sup>+</sup> neutrophils with either a specific β<sub>2</sub>-blocking antibody or an irrelevant antibody. (**Figure 3D and E**). β<sub>2</sub> integrin blockade did not abolish neutrophil slow rolling to VWF at 100s<sup>-1</sup>, showing that Slc44a2/HNA-3a-mediated neutrophil adhesion to VWF is at least partly β<sub>2</sub>-integrin independent. Taken together, these data show that adhesion of HNA-3a<sup>+</sup> neutrophils to VWF is amplified by LPS and doesn't only depend on β<sub>2</sub> integrins, whereas HNA-3b<sup>+</sup> neutrophils does not seem to be affected by LPS in VWF adhesion experiments.

#### Slc44a2/HNA-3b neutrophils are protected from NETosis on VWF at venous shear rates

The enhanced neutrophil adhesion observed for the Slc44a2/HNA-3a<sup>+</sup> group after LPS treatment prompted us to evaluate Slc44a2 involvement in neutrophil activation such as NETosis. NETosis is crucial during VT, and it has been already described in TRALI after antibody binding to HNA-3a following a double “hit” scheme. We reproduced this pattern, priming neutrophils with LPS and modulating an additional factor that could trigger VT. During stasis, local concentrations in leukocytes can increase. We perfused different concentrations of LPS-pre-stimulated neutrophils through a VWF-coated flow chamber. Fluorescence intensity visualization was set-up to focus on cell accumulation and not flowing cells. Cells were flowing normally at the 1.5x10<sup>6</sup> cells/ml concentration in the Ibidi® chambers (**Figure 4A, upper left panel**). However, increasing the perfused cell concentration induced an accumulation of neutrophils (red, calcein red orange) sticking together and to the coated surface. The staining of extracellular DNA (yellow, sytox green) indicates that these neutrophils form NETs, as shown by the presence of DNA fibers escaping from the cells

(**Figure 4A, upper middle and right panels, Suppl. video 3**). This phenomenon was also observed when another chamber brand was used (Cellix®) (**Figure 4A, lower panels, Suppl video 4** after 5 minutes of perfusion **and Suppl video 5** after 15 minutes of perfusion). Co-staining of the cell accumulation at the entrance of the channel for DNA, H3cit and MPO confirmed that these fibers had hallmarks of NETs in both brands of chamber slides (**Figure 4B**). *In vitro* incubation of TNF $\alpha$ -primed HNA-3a<sup>+</sup> neutrophils with VWF resulted in an increase in the percentage of NET-forming cells (**Figure 4C and D**). This supports the hypothesis that Slc44a2/HNA-3a can mediate neutrophil activation and NETosis in presence of VWF.

We performed numerical simulations of the rheological conditions in both chamber brands. We confirmed that the simulated shear rates in contact with the chamber walls of the observation channel are indeed in the desired values, i.e. 100s<sup>-1</sup> (**Figure 5A**). However, flow conditions at the chamber entrance (where the vertical inlet cylindrical channel meets the rectangular section observation channel) show much lower shear rate, toward a few s<sup>-1</sup> (**Figure 5A and 5B**). When compared to the first half of the well this area is characterized by liquid and cells regaining speed (**Figure 5B**). We made digital simulations of cell having made contact with the vertical inlet bottom after 1 minute of cell perfusion. In Cellix® chambers cells are homogeneously deposited at the bottom of the vertical inlet, whereas more cells accumulate there for Ibidi® but mostly at the corner (croissant shape) (**Figure 5C**). Interestingly, we observed that NETosis occurs in this area of low shear, starting more often in the second half part of the vertical inlet bottom (**Figure 5D**). NETosis occurred at lower cell concentration in the Cellix® chamber-entrance, for which the speed of liquid is mostly higher than in the Ibidi® chamber. This suggests from a rheologic perspective that cell speed, cell concentration and a minimal shear stress are essential to observe Slc44a2/VWF-mediated NETosis under flow.

Slc44a2/VWF-mediated NETosis under flow can be amplified by increasing the intensity of the inflammatory stimulus from 5 to 25 $\mu$ g/ml LPS for the two different brands of flow chambers used (**suppl. Figure 3 and Figure 6A**). However, HNA-3b<sup>+</sup> neutrophils did not form extracellular DNA structures (**Figure 6A, right panels**). This HNA-3a-dependent cell accumulation was an all-or-nothing phenomenon (total n=45 channels tested in 5 independent experiments). It was calcium dependent, showing that extracellular DNA trap formation is an active phenomenon following the adhesion of neutrophils to the immobilized VWF under flow. We tested different matrices such as BSA, fibrinogen and VWF-A1 domain and

confirmed to be in the presence of a VWF-A1-dependent phenomenon (**Figure 6B**). These results show that even under inflammatory stimulation, the HNA-3b epitope is protective against NETosis on VWF at venous shear rates *in vitro*.

Slc44a2 plays a major role in neutrophil recruitment at the vessel wall after endothelial degranulation *in vivo*

In order to confirm our data *in vivo*, and because mice “knocked-in” for our polymorphism of interest are not accessible yet, we used *SLC44A2* KO mice and submitted them to the model of histamine-induced endothelial degranulation. Endothelial degranulation results in VWF release from the Weibel-Palade bodies. Mouse infusion with fluorescently labeled anti-Ly-6G antibody allowed us to track neutrophil accumulation at the vessel wall in this model. Our data confirmed our *in vitro* hypothesis: we observed a drastic reduction in neutrophil rolling and adhesion at the vessel wall of mesenteric venules in absence of Slc44a2 (**Figure 7**,  $409 \pm 300$  cells/min versus  $59 \pm 26$  cells/min).

## Discussion

In the present study, we demonstrated that Slc44a2 is involved in the direct adhesion and activation process of neutrophils on VWF. Slc44a2-mediated adhesion and NETosis are HNA 3a/HNA-3b- and VWF-A1 domain-dependent. These phenomena are potentialized by inflammatory stimulation, low shear rates ( $100\text{s}^{-1}$ ) and cell concentration.

GWAS studies have homogeneously identified *SLC44A2* as a new gene associated with VT risk. This was reinforced by mice data we and others obtained showing that absence of Slc44a2 is linked to reduced thrombus formation in the stenosis VT model.<sup>4,5</sup> Until these findings, pathophysiology of VT was mostly based on the original cascade model of coagulation. Because Slc44a2 does not belong to it, it is of major importance to characterize the biological link between this protein and VT. In the current study, we aimed to understand how the *SLC44A2* gene and the lead rs2288904 variant (461G>A; Arg154Gln; HNA-3a/HNA-3b) could affect Slc44a2 function in thrombosis through neutrophils. This last decade, neutrophils and VWF have been shown to play a central role in VT.<sup>17,20,25</sup> VWF is known to be an important protein in hemostasis by mediating platelet adhesion to the subendothelial matrix, but also in inflammation processes (for review<sup>26</sup>) that are crucial during VT development. Slc44a2 has been previously shown as a binding partner for VWF.<sup>10</sup> However, how the Arg154Gln polymorphism could directly modulate cell interaction with VWF at low shear rates had not been studied. Constantinescu-Bercu *et al.* recently published a paper showing that Slc44a2 could permit adhesion of neutrophil to primed platelets adhered at high shear rates ( $1000\text{s}^{-1}$ ) on VWF via their  $\alpha_{\text{IIb}}\beta_3$  receptors.<sup>11</sup> ~~However, platelets are not the crucial players in VT.~~ It is indeed possible that neutrophils do not need platelets to bind the VWF-A1 domain as suggested originally by Bayat *et al.*<sup>10</sup> A very recent work suggested that Slc44a2 could regulate platelet mitochondrial function thus affecting platelet ADP production.<sup>5</sup> The fact that VWF and neutrophils are essential in VT does not necessarily mean that platelets are essential to recruit neutrophil at the endothelium even if they participate in the process.

Because HNA-3b expression is associated with a decreased risk for VT in patients,<sup>1,2</sup> we imagined a possible loss of function of Slc44a2/HNA-3b leading to a reduced binding of Slc44a2 to VWF. We used HEK293T transfected cells, neutrophils and mice to assess Slc44a2 importance in the mechanisms of neutrophil adhesion to VWF *in vitro* and *in vivo*. We observed that the HNA-3a/HNA-3b epitope had no effect on neutrophil rolling ( $200\text{--}500\mu\text{m/s}$ ) when perfused on a VWF-coated matrix. However, our data show that

Slc44a2/HNA-3a but not Slc44a2/HNA-3b is crucial for HEK293T or neutrophil “slow rolling” (0-10 $\mu$ m/s) to VWF at venous shear rates (100s<sup>-1</sup>).

When looking at our rolling data we must consider that 2% of total tracked cells in “slow rolling” for the HNA-3a group can be relevant. The majority (60-75%) of the total tracked cells are non-sedimented (not close enough to the wall). MnCl<sub>2</sub>/calcium was used as positive control to determine the maximal percentage of neutrophils in “slow rolling”. MnCl<sub>2</sub> forces integrins to stay in their active conformation, maximizing cell adhesion on an integrin substrate such as VWF. 28%  $\pm$  8% of the total cells were observed in this positive control group representing the 100% slow rolling/adhesion (**Suppl Fig 2**). Moreover our *in vivo* data confirm that Slc44a2 play a significant role in neutrophil recruitment at the vessel wall in mice.

Despite the fact that HEK293T/HNA-3a cells do not express  $\beta_2$ -integrins,<sup>27</sup> they adhere more on VWF than HEK293T/HNA-3b cells. However, subsequent integrin activation could potentialize Slc44a2-mediated adhesion of neutrophils as integrins have been described as playing a major role in leukocyte adhesion.<sup>28</sup> The utilization of a  $\beta_2$ -blocking antibody on neutrophils was not enough to abolish neutrophil adhesion on VWF. Altogether these observations confirm that Slc44a2 is enough to induce cell adhesion on VWF under flow at least independently from integrins. However, we cannot exclude that  $\beta_2$  integrins are not involved further in the process of neutrophil recruitment to VWF. Indeed, our results and previous findings<sup>10</sup> suggest that VWF/Slc44a2 interaction could induce neutrophil and integrin activation thus consolidating the cell adhesion process. In TRALI for instance, anti-HNA-3a antibodies have been shown to activate neutrophils.<sup>14</sup> VWF may have a comparable effect. Bayat and collaborators published evidence that following VWF binding to Slc44a2, VWF, Slc44a2, and Mac-1 ( $\alpha_M\beta_2$ ) form a trimolecular complex at the neutrophil surface.<sup>10</sup> In addition, the work from Constantinescu-Bercu *et al.* points out that Slc44a2 engagement with  $\alpha_{IIb}\beta_3$  could induce Slc44a2-mediated signaling that participates in neutrophil integrin activation. These observations can lead us to expect an “inside-out” signaling. We observed that neutrophils purified from EDTA-anticoagulated blood showed even less adhesion on VWF than neutrophils after  $\beta_2$ -blockade (data not shown). Chelation of divalent cations may affect a possible Slc44a2-mediated calcium mobilization involved in the adhesion process. An old study has also identified the Slc44a2-coding gene as able to activate the NF- $\kappa$ B pathway.<sup>29</sup> Interestingly, this pathway is essential for tissue factor expression in VT.<sup>30</sup>

We have seen that a second hit can significantly affect Slc44a2-mediated neutrophil slow rolling to VWF under flow. In order to track cells upon LPS activation we used a dye

incorporating membranes. This dye may have further contributed to cell activation. The dye effect was dose-dependent (data not shown), and it increased the rolling background of HNA-3a and HNA-3b neutrophils.

HNA-3a expression, but also special rheological conditions or additional inflammatory stimuli (such as TNF- $\alpha$  or LPS) can stimulate NETosis. We thus tested different dyes for NETosis observation (such as anti-Ly6g-antibodies and Calcein) to exclude some dye-dependent artefact. The fact that HNA-3b<sup>+</sup> neutrophils are protected from increased adhesion and activation on VWF despite LPS-activation supports our two-hit-hypothesis where cells need two priming events to present a pro-inflammatory profile. These results complete observations from the work of Constantinescu-Bercu *et al.* that showed that neutrophils formed NETs when adhered to platelets through the  $\alpha_{IIb}\beta_3$  integrin<sup>11</sup> and suggest that Slc44a2 could be a mechanosensor able to modulate cell activation in response to flow. NETosis is an active process following neutrophil activation, crucial during VT.<sup>18,20</sup> NETs form a matrix for cell (platelets, red blood cells)<sup>31</sup> or microparticle adhesion<sup>32</sup> and represent a thrombogenic surface exposing tissue factor<sup>33</sup> or factor XII.<sup>18</sup>

Our *in vivo* results obtained in the histamine-induced endothelial degranulation model in mice support that Slc44a2 deficiency could delay both neutrophil recruitment and activation on a degranulated endothelium too. This may explain the phenotype of *SLC44A2* KO mice that formed smaller thrombi when submitted to the DVT stenosis model.<sup>4</sup>

VWF and NETs are crucial in VT pathogenesis. It is also true for other pathologies linked to inflammation such as stroke or myocardial ischemia/reperfusion injury.<sup>34-37</sup> HNA-3a has also been associated with stroke.<sup>2</sup> Stroke involves the VWF-A1 domain,<sup>38</sup> which is the one important in Slc44a2-mediated adhesion as well. Our work suggests that GPIb may not be the only receptor involved when we talk about VWF-A1-associated thrombo-inflammatory pathogenesis. Slc44a2 has to be taken into consideration. Also, it is not excluded that Slc44a2 could bind the same part of the VWF-A1 domain than the platelet GPIb receptor. VWF is released by endothelial cells through a constitutive pathway and through Weibel-Palade bodies release. VWF released from the storage compartment is of high molecular weight<sup>39</sup> and is released with a relatively high concentrations of calcium ions<sup>40</sup> upon vascular injury or inflammatory stimulation. Our work suggests that Slc44a2 may be involved not only in VT but also in more pathologies than we originally thought in the inflammation field.

HNA-3b homozygous individuals being rare (6% of Caucasians),<sup>22</sup> it is easy to imagine that previous work focusing on neutrophil adhesion and VWF used HNA-3a-positive donors. Here we point out the necessity to check on the HNA-3a/3b genotype of blood donors before working with VWF.

This paper presents some limitations. The flow chambers used in this study do not exactly mimic human veins: they are devoid of vein valves (no valve-associated flow disturbances), wall plasticity and pulsatile blood flow. Our system does not include other blood cells which can possibly potentialize interactions. However, this model allowed us to determine in a simple calibrated system how Slc44a2 impacts by itself neutrophil cell velocity on a VWF matrix. We could determine the effect of shear rates, cell concentration, inflammatory pre-stimulation and observe NETosis in specific rheologic condition. The use of LPS to mimic inflammation does not reflect sterile inflammation but infection-related inflammation. We only used male mice of young age (12-week-old). Venous thrombosis is not gender exclusive. However, it allowed us to reduce data variability that could have been influenced by female estrous cycles. Despite the fact that the age is important to study age-related thrombosis, to have young mice with less abdominal fat allowed us to study the involvement of a protein in a physiological process.

In conclusion, we propose a new mechanism of neutrophil adhesion and activation that connects inflammation to thrombosis in veins. This mechanism involves the VWF-A1 domain and can induce neutrophil activation and NETosis. Other studies are thus warranted to better understand the mechanisms of Slc44a2/VWF molecular interaction and how this interaction can also influence neutrophil activation. Slc44a2 being expressed by neutrophils, platelets and endothelial cells, it would be interesting to determine the relative contribution of Slc44a2 from these cells in thrombo-inflammatory disorders. Shutting down Slc44a2 function would allow to target specifically thrombosis without affecting hemostasis, which would reduce the risk of hemorrhagic complications that are associated with actual prophylactic anticoagulant therapies.

## Acknowledgments

The authors thank Thomas E. Carey (Kresge Hearing Research Institute, Department of Otolaryngology/Head and Neck Surgery, University of Michigan, Ann Arbor, MI, USA) for the floxed *SLC44A2* mouse embryos used to generate the mice on a C57BL/6J background<sup>3</sup>; Michel Grino, Matthias Canault, Cécile Denis for helpful discussions; and Brian Curtis, Daniel Bougie for providing us with the HEK293T transfected cells. This work was supported by Trombosestichting Nederland (#2015-4) and the ANR (grant ANR-17-CE14-0003-01 (G.M.T)).

## Author contributions

Experimental design: GZ, PR, BJMvV, MCA, P JL, PEM, GMT. Performed experiments and analyzed data: GZ, JT, PR, VT, CXM, PL, BJMvV, MCA, P JL, PEM, GMT. Wrote the paper: GZ, PR, PEM and GMT. All authors commented on manuscript drafts. All authors have approved the final version.

## Disclosure of Conflicts of Interest

The authors declare no competing financial interests.

**Data sharing:** To access data and protocols, contact the corresponding author, grace.thomas@univ-amu.fr.

## References

1. Germain M, Chasman DI, de Haan H, et al. Meta-analysis of 65,734 individuals identifies TSPAN15 and SLC44A2 as two susceptibility loci for venous thromboembolism. *Am. J. Hum. Genet.* 2015;96(4):532–542.
2. Hinds DA, Buil A, Ziemek D, et al. Genome-wide association analysis of self-reported events in 6135 individuals and 252 827 controls identifies 8 loci associated with thrombosis. *Hum. Mol. Genet.* 2016;25(9):1867–1874.
3. Tilburg J, Adili R, Nair TS, et al. Characterization of hemostasis in mice lacking the novel thrombosis susceptibility gene Slc44a2. *Thrombosis Research.* 2018;171:155–159.
4. Tilburg J, Coenen DM, Zirka G, et al. SLC44A2 deficient mice have a reduced response in stenosis but not in hypercoagulability driven venous thrombosis. *Journal of Thrombosis and Haemostasis.* 2020;18(7):1714–1727.
5. Bennett JA, Mastrangelo MA, Ture SK, et al. The choline transporter Slc44a2 controls platelet activation and thrombosis by regulating mitochondrial function. *Nature Communications.* 2020;11(1):3479.
6. Greinacher A, Wesche J, Hammer E, et al. Characterization of the human neutrophil alloantigen-3a. *Nat. Med.* 2010;16(1):45–48.
7. Curtis BR, Sullivan MJ, Holyst MT, et al. HNA-3a-specific antibodies recognize choline transporter-like protein-2 peptides containing arginine, but not glutamine at Position 154. *Transfusion.* 2011;51(10):2168–2174.
8. Kanack AJ, Peterson JA, Sullivan MJ, et al. Full-length recombinant choline transporter-like protein 2 containing arginine 154 reconstitutes the epitope recognized by HNA-3a antibodies. *Transfusion.* 2012;52(5):1112–1116.
9. Flesch BK, Wesche J, Berthold T, et al. Expression of the CTL2 transcript variants in human peripheral blood cells and human tissues. *Transfusion.* 2013;53(12):3217–3223.
10. Bayat B, Tjahjono Y, Berghöfer H, et al. Choline Transporter-Like Protein-2: New von Willebrand Factor-Binding Partner Involved in Antibody-Mediated Neutrophil Activation and Transfusion-Related Acute Lung Injury. *Arterioscler. Thromb. Vasc. Biol.*

2015;35(7):1616–1622.

11. Constantinescu-Bercu A, Grassi L, Frontini M, et al. Activated  $\alpha$ IIB $\beta$ 3 on platelets mediates flow-dependent NETosis via SLC44A2. *eLife*. 2020;9:.
12. Mair DC, Eastlund T. The pathophysiology and prevention of transfusion-related acute lung injury (TRALI): a review. *Immunohematology*. 2010;26(4):161–173.
13. Berthold T, Muschter S, Schubert N, et al. Impact of priming on the response of neutrophils to human neutrophil alloantigen-3a antibodies. *Transfusion*. 2015;55(6 Pt 2):1512–1521.
14. Thomas GM, Carbo C, Curtis BR, et al. Extracellular DNA traps are associated with the pathogenesis of TRALI in humans and mice. *Blood*. 2012;119(26):6335–6343.
15. Caudrillier A, Kessenbrock K, Gilliss BM, et al. Platelets induce neutrophil extracellular traps in transfusion-related acute lung injury. *J. Clin. Invest*. 2012;122(7):2661–2671.
16. Darbousset R, Thomas GM, Mezouar S, et al. Tissue factor-positive neutrophils bind to injured endothelial wall and initiate thrombus formation. *Blood*. 2012;120(10):2133–2143.
17. Brill A, Fuchs TA, Savchenko AS, et al. Neutrophil extracellular traps promote deep vein thrombosis in mice. *J. Thromb. Haemost*. 2012;10(1):136–144.
18. von Bruhl M-L, Stark K, Steinhart A, et al. Monocytes, neutrophils, and platelets cooperate to initiate and propagate venous thrombosis in mice in vivo. *J. Exp. Med*. 2012;209(4):819–835.
19. Fuchs TA, Brill A, Wagner DD. Neutrophil extracellular trap (NET) impact on deep vein thrombosis. *Arterioscler. Thromb. Vasc. Biol*. 2012;32(8):1777–1783.
20. Martinod K, Demers M, Fuchs TA, et al. Neutrophil histone modification by peptidylarginine deiminase 4 is critical for deep vein thrombosis in mice. *Proc. Natl. Acad. Sci. U.S.A.* 2013;110(21):8674–8679.
21. Bougie DW, Peterson JA, Kanack AJ, Curtis BR, Aster RH. Transfusion-related acute lung injury-associated HNA-3a antibodies recognize complex determinants on choline transporter-like protein 2. *Transfusion*. 2014;54(12):3208–3215.
22. Bowens KL, Sullivan MJ, Curtis BR. Determination of neutrophil antigen HNA-3a and HNA-3b genotype frequencies in six racial groups by high-throughput 5' exonuclease assay. *Transfusion*. 2012;52(11):2368–2374.
23. Wang P, Wu P, Anthes JC, et al. Interleukin-10 inhibits interleukin-8 production in human neutrophils. *Blood*. 1994;83(9):2678–2683.
24. Fuchs TA, Abed U, Goosmann C, et al. Novel cell death program leads to neutrophil extracellular traps. *J. Cell Biol*. 2007;176(2):231–241.
25. Brill A, Fuchs TA, Chauhan AK, et al. von Willebrand factor-mediated platelet adhesion is critical for deep vein thrombosis in mouse models. *Blood*. 2011;117(4):1400–1407.
26. Kawecki C, Lenting PJ, Denis CV. von Willebrand factor and inflammation. *Journal of Thrombosis and Haemostasis*. 2017;15(7):1285–1294.
27. Gupta V, Alonso JL, Sugimori T, et al. Role of the  $\beta$ -Subunit Arginine/Lysine Finger in Integrin Heterodimer Formation and Function. *The Journal of Immunology*. 2008;180(3):1713–1718.
28. Kuijpers TW, Van Lier RA, Hamann D, et al. Leukocyte adhesion deficiency type 1 (LAD-1)/variant. A novel immunodeficiency syndrome characterized by dysfunctional beta2 integrins. *J. Clin. Invest*. 1997;100(7):1725–1733.
29. Matsuda A, Suzuki Y, Honda G, et al. Large-scale identification and characterization of human genes that activate NF-kappaB and MAPK signaling pathways. *Oncogene*. 2003;22(21):3307–3318.
30. Li Y-D, Ye B-Q, Zheng S-X, et al. NF-kappaB transcription factor p50 critically regulates tissue factor in deep vein thrombosis. *J. Biol. Chem*. 2009;284(7):4473–4483.
31. Fuchs TA, Brill A, Duerschmied D, et al. Extracellular DNA traps promote

thrombosis. *Proc. Natl. Acad. Sci. U.S.A.* 2010;107(36):15880–15885.

32. Thomas GM, Brill A, Mezouar S, et al. Tissue factor expressed by circulating cancer cell-derived microparticles drastically increases the incidence of deep vein thrombosis in mice. *J. Thromb. Haemost.* 2015;13(7):1310–1319.

33. Kambas K, Chrysanthopoulou A, Vassilopoulos D, et al. Tissue factor expression in neutrophil extracellular traps and neutrophil derived microparticles in antineutrophil cytoplasmic antibody associated vasculitis may promote thromboinflammation and the thrombophilic state associated with the disease. *Ann. Rheum. Dis.* 2014;73(10):1854–1863.

34. Zhao B-Q, Chauhan AK, Canault M, et al. von Willebrand factor-cleaving protease ADAMTS13 reduces ischemic brain injury in experimental stroke. *Blood.* 2009;114(15):3329–3334.

35. Hillgruber C, Steingraber AK, Pöppelmann B, et al. Blocking Von Willebrand Factor for Treatment of Cutaneous Inflammation. *Journal of Investigative Dermatology.* 2014;134(1):77–86.

36. Savchenko AS, Borissoff JJ, Martinod K, et al. VWF-mediated leukocyte recruitment with chromatin decondensation by PAD4 increases myocardial ischemia/reperfusion injury in mice. *Blood.* 2014;123(1):141–148.

37. Dhanesha N, Prakash P, Doddapattar P, et al. Endothelial Cell-Derived von Willebrand Factor Is the Major Determinant That Mediates von Willebrand Factor-Dependent Acute Ischemic Stroke by Promoting Postischemic Thrombo-Inflammation. *Arterioscler. Thromb. Vasc. Biol.* 2016;36(9):1829–1837.

38. Denorme F, Martinod K, Vandenbulcke A, et al. The von Willebrand Factor A1 domain mediates thromboinflammation, aggravating ischemic stroke outcome in mice. *Haematologica.* 2020;haematol.2019.241042.

39. Wagner DD. Cell biology of von Willebrand factor. *Annu. Rev. Cell Biol.* 1990;6:217–246.

40. Poisner A, Trifaro J-M. Common properties in the mechanisms of synthesis, processing and storage of secretory products. *The Secretory Granule.* 1982.

## Figure legends

### **Figure 1. HEK293T/HNA-3a cells bind more to VWF than HEK293T/HNA-3b cells.**

Quantification of maximal fluorescence intensity recorded per cell and representing anti-VWF staining on transfected HNA-3a- (grey circle) or HNA-3b-expressing HEK293T cells (white triangle). Each dot represents a separate cell with n= 81,153, 72 and 80 cells analyzed respectively for HNA-3a-VWF, HNA-3a+VWF, HNA-3b-VWF and HNA-3b+VWF groups (Mean±SEM, one-way ANOVA test, \*\*\* p<0.005).

### **Figure 2. The Slc44a2/HNA-3a epitope is necessary for cell slow rolling to VWF under flow.**

(A, C) Compiled amount of HEK293T cells (n=5 independent experiments) (A) or neutrophils (HNA-3a n=6 donors; HNA-3b n=3 donors) (C) counted in function of their mean velocity ( $\mu\text{m/s}$ ) on coated VWF when submitted to a  $100\text{s}^{-1}$  shear rate. The dashed line separates sedimented (left) from non-sedimented cells (right). Red: HNA-3a-expressing cells; black: HNA-3b-expressing cells). (B, D and E) Graphs depicting the “slow rolling” and “rolling” profiles of HEK293T cells (B) and neutrophils (D, E) perfused on a VWF matrix under flow at a  $100\text{s}^{-1}$  shear rate. Perfusion of cells at  $100\text{s}^{-1}$  resulted in more slow rolling of Slc44a2/HNA-3a-expressing HEK293T cells (B, n=5 independent experiments) and neutrophils (D, HNA-3a n=6 donors; HNA-3b n=3 donors) to human VWF coated channels compared to Slc44a2/HNA-3b expressing cells. Slow rolling and rolling of Slc44a2/HNA-3a expressing neutrophils (E, n=7 donors) to VWF were blocked by VWF-A1 domain blocking monoclonal antibody. Data represented in nested form: values obtained for each field are shown. 3 fields were analyzed for each experiment/donor ((A, C) Mean±SEM; (B, C, D) nested t-test, min/max, quartiles and medians are represented; \* p<0.05; \*\* p<0.01; \*\*\* p<0.005)

### **Figure 3. Adhesion of HNA-3a-expressing neutrophils to VWF is amplified by LPS and does not require $\beta_2$ integrins.**

(A) Percentage of total tracked neutrophils qualified as in “slow rolling” when perfused at  $100\text{s}^{-1}$ ,  $50\text{s}^{-1}$  and  $10\text{s}^{-1}$  on immobilized VWF (HNA-3a: n=6 donors per condition; HNA-3b: n=6 donors for  $100\text{s}^{-1}$  and 5 donors for  $50\text{s}^{-1}$  and  $10\text{s}^{-1}$ ). (B, C) Percentage of total tracked neutrophils qualified as in “slow rolling” (B) and in “rolling” (C) when perfused at  $100\text{s}^{-1}$  on immobilized VWF after LPS treatment ( $5\mu\text{g/ml}$  or  $25\mu\text{g/ml}$ ) prior to perfusion (n=5 donors per condition). (D, E) Percentage of total tracked neutrophils qualified as in “slow rolling” (D) and in “rolling” (E) when perfused at  $100\text{s}^{-1}$  on immobilized VWF after treatment with a

$\beta_2$  integrin blocking IgG, or a control irrelevant IgG (HNA-3a: n=4 donors; HNA-3b: 3 donors per condition). Data are represented in nested form: values obtained for each field are shown, 3 fields were analyzed for each experiment/donor (Min/max, quartiles and medians are represented; nested t-test; \*  $p<0.05$ ; \*\*  $p<0.01$ ).

**Figure 4. Primed neutrophils in contact with VWF can form DNA extracellular traps.**

(A) Representative images of fluorescently labeled LPS-primed neutrophils (PMN, red) and extracellular DNA (exDNA, yellow) after perfusion ( $100\text{s}^{-1}$  shear rate) on VWF of different concentrations of neutrophils in two different brands of flow chambers (n=2 donors per chamber brand). Dashed lines have been added for more convenience to delimit the flow channels and the well entrance. (B) Representative images of fluorescently-labeled NETs at the chamber entrance showing total DNA (Hoechst 33342, blue), H3cit (green) and MPO (pink) staining after perfusion of neutrophils in Ibidi® slides at  $24 \times 10^6$  cells/ml (upper panel, n=3 donors and 9 channels) and in Cellix® slides at  $1.5 \times 10^6$  cells/ml (lower panel, n=2 donors and 4 channels) (C-D) Quantification of NETs after VWF challenge by fluorescence microscopy analysis. HNA-3a<sup>+</sup> neutrophils were primed with TNF $\alpha$  (to mimic LPS activation) and incubated for 180 minutes with PBS (+TNF $\alpha$ ) or VWF (+TNF $\alpha$ +VWF). DNA release was visualized after DNA staining with Hoescht 33342 (n=9 fields/well, 3 wells/condition, 2 independent experiments) (Mean $\pm$ SD; \*\*\*  $p<0.005$ ). (D) Representative fluorescence images from quantifications shown in panel (C). Scale bar=100  $\mu\text{m}$

**Figure 5. Numerical simulations of rheological conditions and cell motion in chamber entrance.**

(A) Maps of shear rate at chamber bottom wall for Cellix® chamber for flow of  $4\mu\text{l}/\text{min}$  (left panel) and for Ibidi® chamber for flow of  $10\mu\text{l}/\text{min}$  (right panel) corresponding experimentally to a desired shear rate of  $100\text{s}^{-1}$  in the observation section of the chamber. Scale bar = 200 $\mu\text{m}$ . (B) Map of fluid and cell velocity in a sagittal cut of the Cellix® chamber (left panel) or the Ibidi® chamber entrance (right panel) along its symmetry axis. Cells are simulated as spheres. (C) Number of deposited cells at t=60sec as a function of the cell concentration perfused into the chambers. (D) Representative images of fluorescently labeled neutrophils (Ly6G, pink) and extracellular DNA (exDNA, green) after perfusion ( $100\text{s}^{-1}$  shear rate) on VWF in a Cellix® flow chamber (n=3). Scale bar=100  $\mu\text{m}$ . Dashed lines have been added to delimit the flow channels and the well entrance.

**Figure 6. Neutrophil activation on VWF at  $100\text{s}^{-1}$  is HNA-3a-, calcium-, VWF A1-**

**domain-dependent, and can be exacerbated by LPS challenge.**

(A) Representative images of HNA-3a- or HNA-3b neutrophils (anti-Ly6G IgG) submitted to a  $100\text{s}^{-1}$  shear rate in absence or presence of calcium, or pre-activated with LPS prior to perfusion (5 or  $25\mu\text{g/ml}$ ) (Cellix® flow chambers, n=3 donors per genotype). (B) Representative images of HNA-3a neutrophils perfused at a  $100\text{s}^{-1}$  shear rate on immobilized BSA, fibrinogen or VWF A1-Fc domain. Neutrophil Fc receptors were blocked with anti CD32 antibody for A1 domain experiments. Scale bar= $100\mu\text{m}$ . Lines delimit the flow channels and the well entrance (n=3 donors per genotype).

**Figure 7. Slc44a2 is essential for neutrophil recruitment at the vessel wall following endothelial activation.**

Intravital microscopy was performed on mesenteric venules of mice deficient in Slc44a2 protein (*SLC44A2* KO mice) after IP histamine challenge. (A) Quantification of neutrophil rolling on mesenteric venules in wild-type (WT) and *SLC44A2* KO mice (WT, n=7 venules in 3 mice; *SLC44A2* KO, n=8 venules in 3 mice). (B) Representative images showing reduced neutrophil recruitment in mesenteric venules of *SLC44A2* KO mice after staining of endogenous rolling neutrophils by infusion of an Alexa 660-anti-Ly6g antibody. (bars represent means; \*  $p<0.05$ ). Scale bar= $100\mu\text{m}$ .

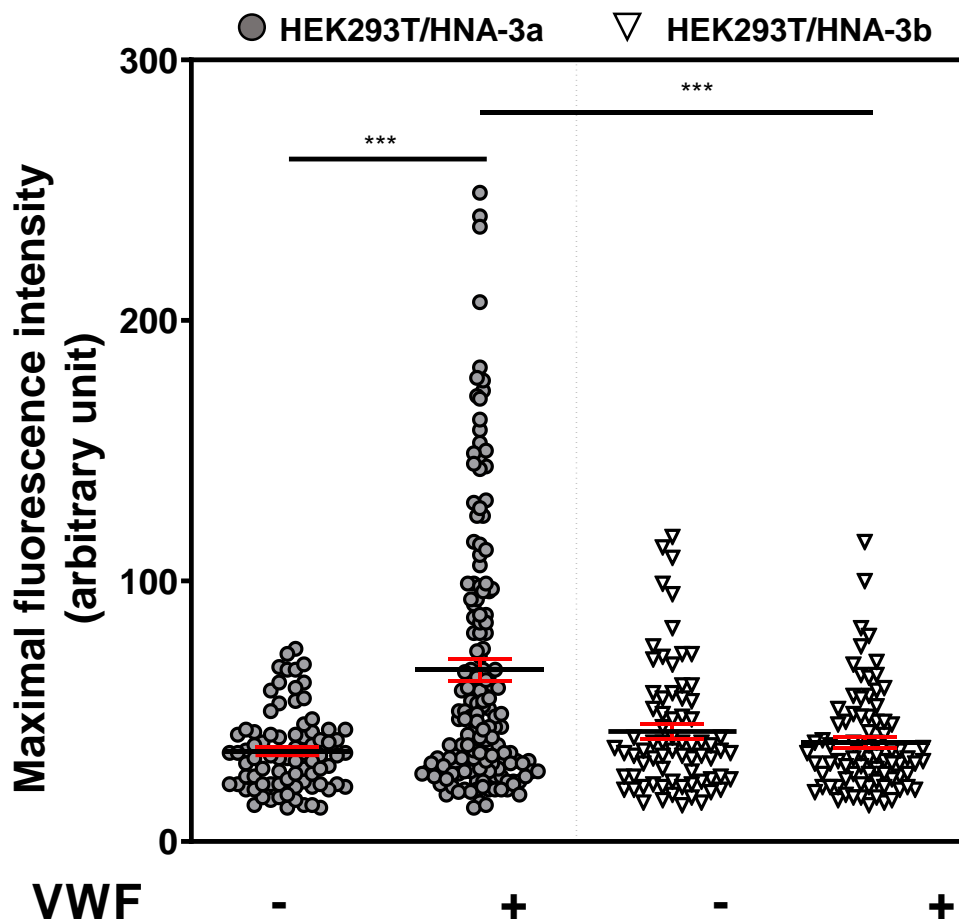
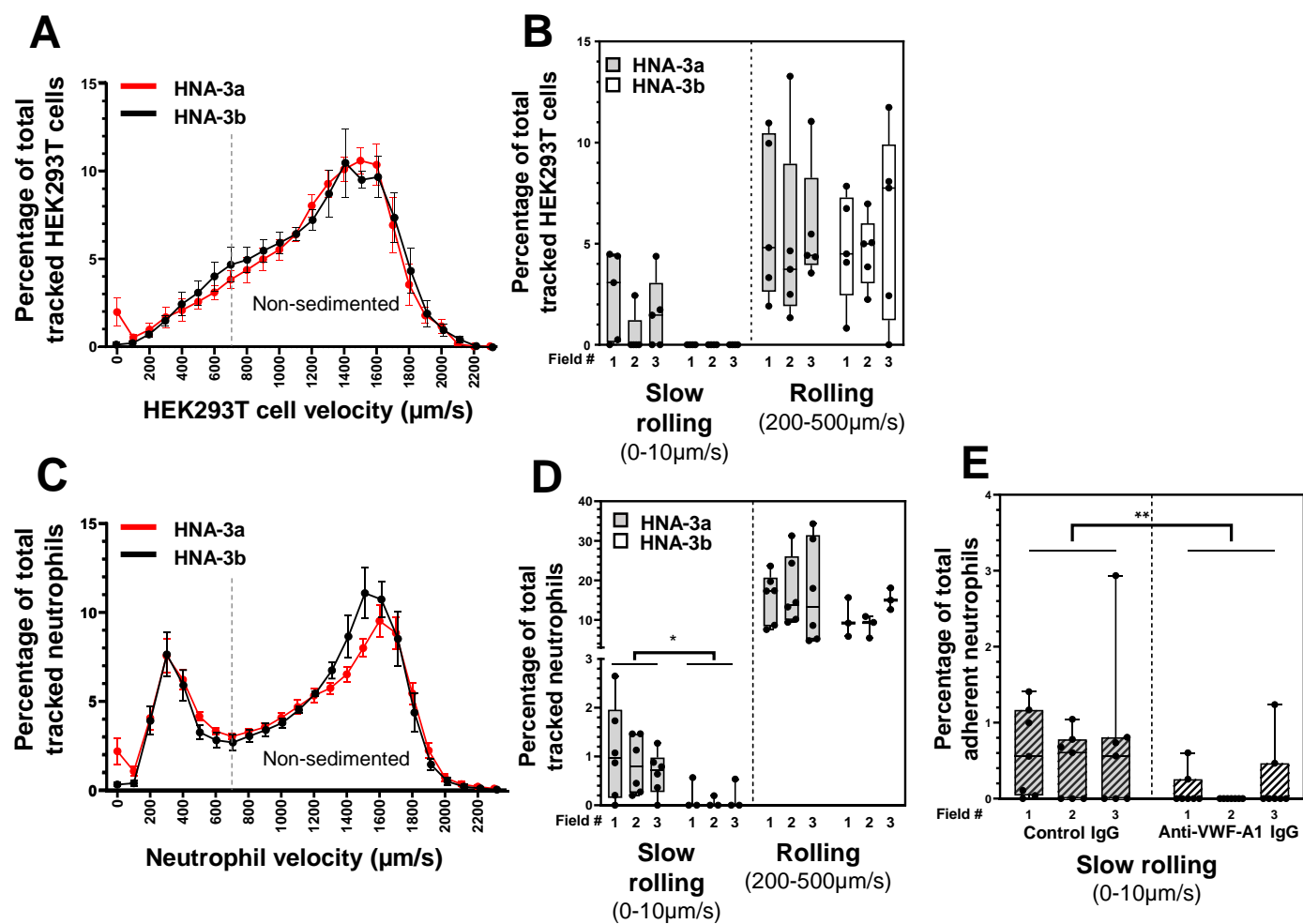
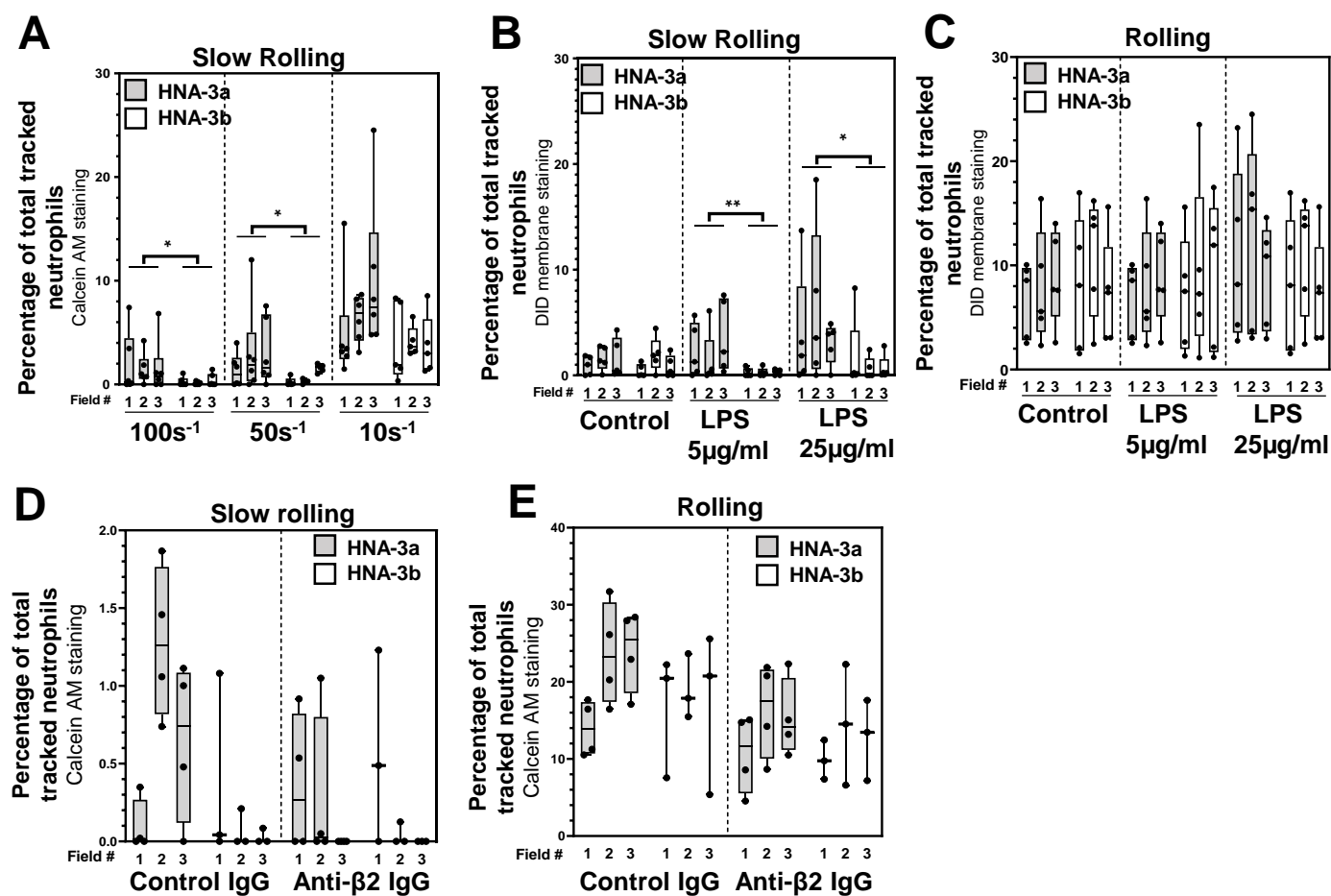


Figure 1. HEK293T/HNA-3a cells bind more to VWF than HEK293T/HNA-3b cells.



**Figure 2. The Slc44a2/HNA-3a epitope is necessary for cell slow rolling to VWF under flow.**



**Figure 3. Adhesion of HNA-3a-expressing neutrophils to VWF is amplified by LPS and does not require  $\beta_2$  integrins.**

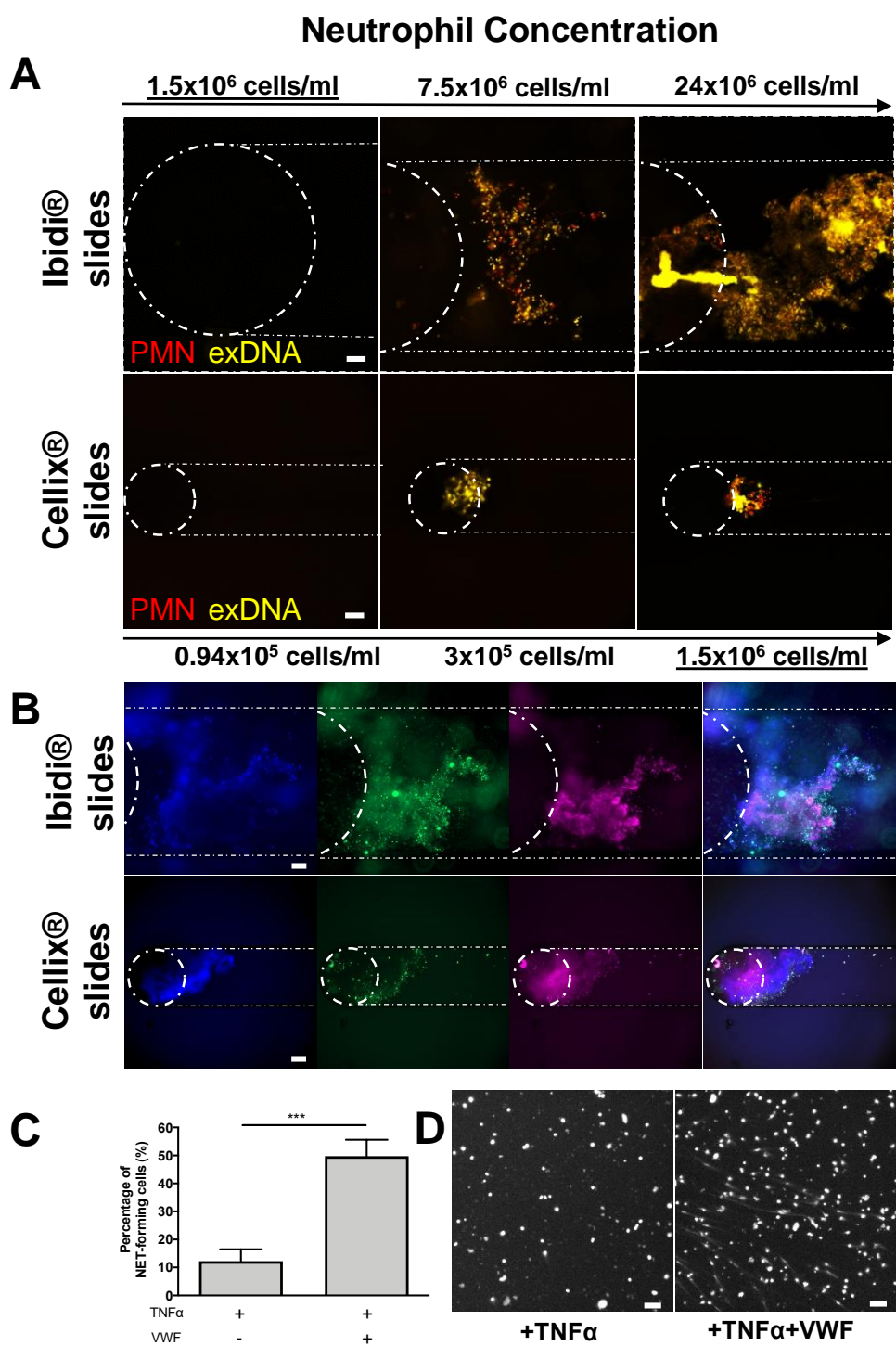


**Figure 4. Primed neutrophils in contact with VWF can form DNA extracellular traps.**

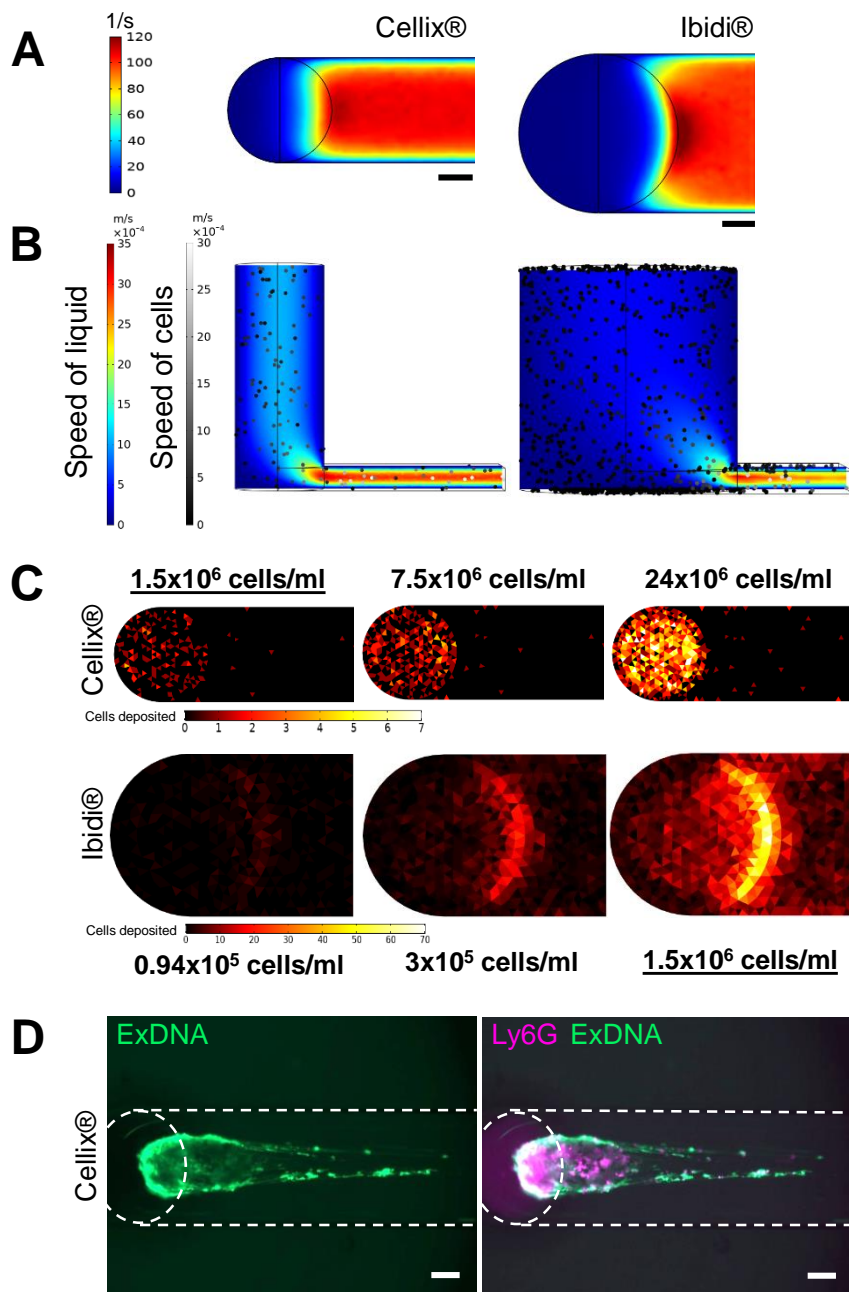


**Figure 5. Numerical simulations of rheological conditions and cell motion in chamber entrance.**

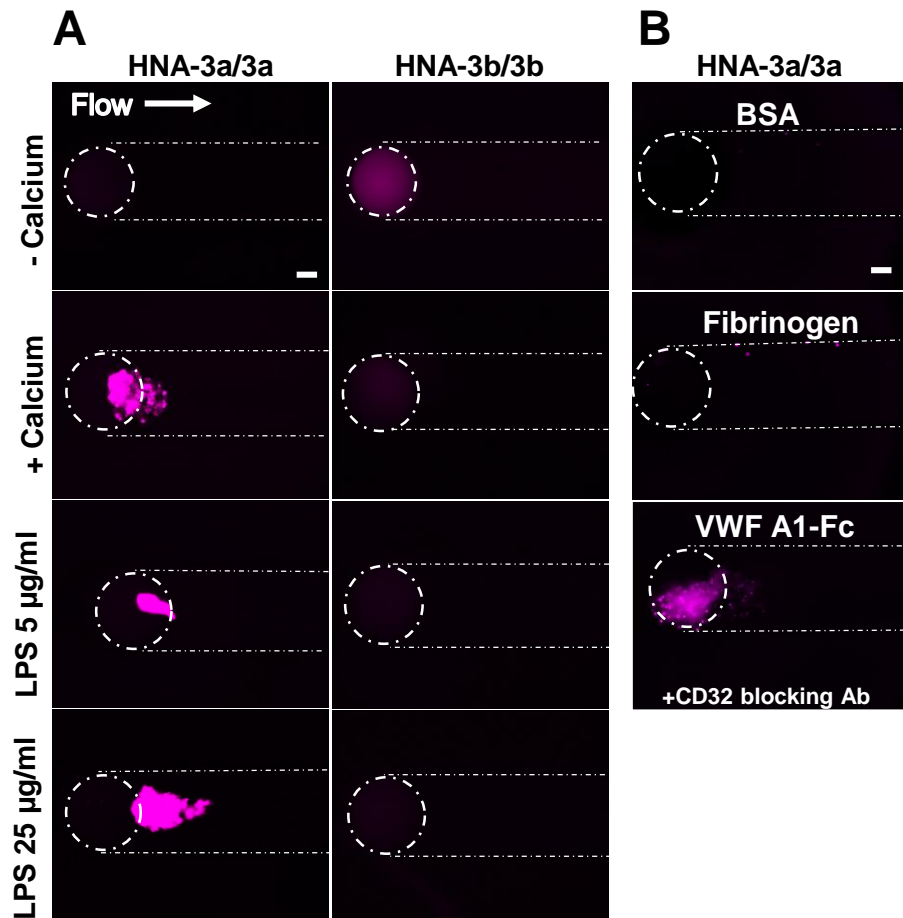


**Figure 6. Neutrophil activation on VWF at  $100\text{s}^{-1}$  is HNA-3a-, calcium-, VWF A1-domain-dependent, and can be exacerbated by LPS challenge.**

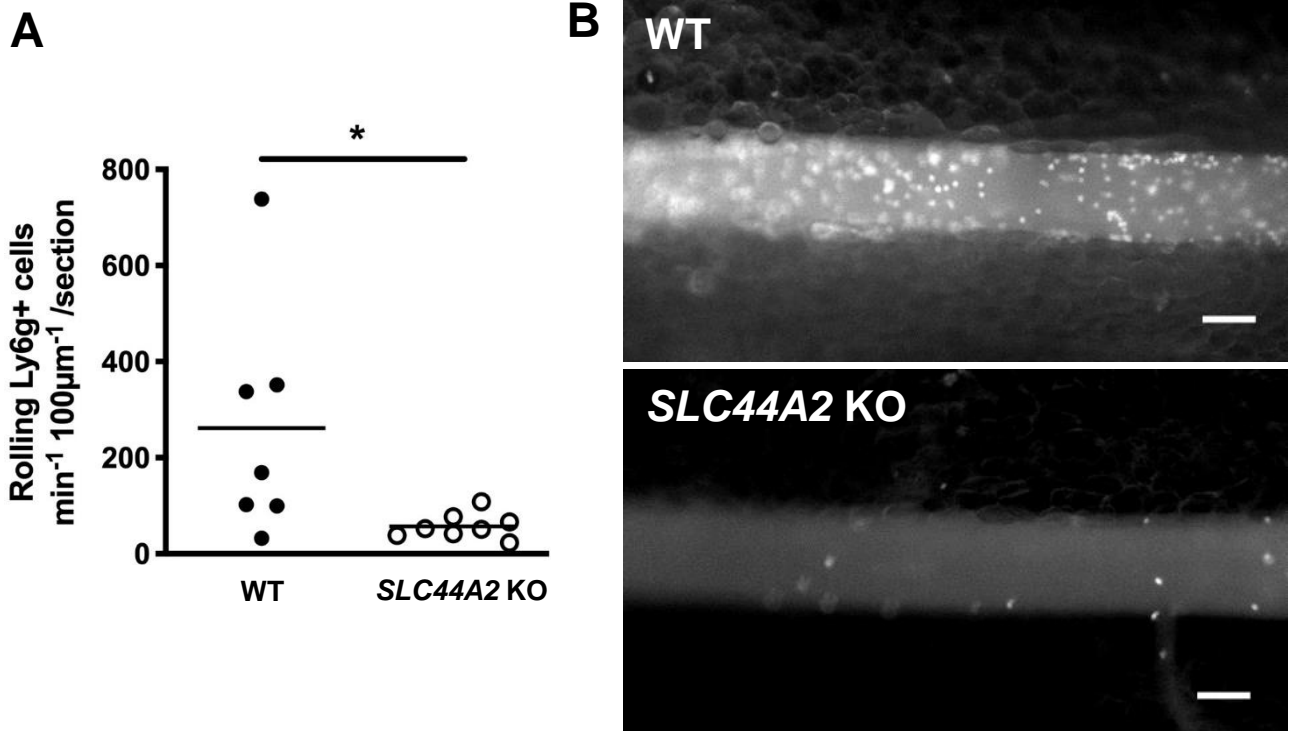


**Figure 7. Slc44a2 is essential for neutrophil recruitment at the vessel wall following endothelial activation.**